


## Layer-coherent phase in double-layer graphene at $\nu_1 = \nu_2 = 0$

Amartya Saha<sup>1,\*</sup> and Ankur Das<sup>2,†</sup><sup>1</sup>*Department of Physics and Astronomy, University of Kentucky, Lexington, Kentucky 40506, USA*<sup>2</sup>*Department of Condensed Matter Physics, Weizmann Institute of Science, Rehovot 76100, Israel*
 (Received 28 March 2021; revised 3 October 2021; accepted 16 December 2021; published 5 January 2022)

In the recent advancement in graphene heterostructures, it is possible to create a double-layer tunnel decoupled graphene system that has a strong interlayer electronic interaction. In this work, we restrict the parameters in the low energy effective Hamiltonian using simple symmetry arguments. Then, we study the ground state of this system in the Hartree-Fock approximation at  $\nu_1 = \nu_2 = 0$ . In addition to the phases found in monolayer graphene, we found an existence of layer-coherent phase which breaks the layer  $U(1)$  symmetry. At nonzero Zeeman coupling strength ( $E_z$ ), this layer-coherent state has a small magnetization that vanishes when  $E_z$  tends to zero. We discuss the bulk gapless modes using the Goldstone theorem. We also comment on the edge structure for the layer-coherent phase.

DOI: [10.1103/PhysRevB.105.035405](https://doi.org/10.1103/PhysRevB.105.035405)

### I. INTRODUCTION

After the discovery of the quantum Hall effect in two dimensional electron gas (2DEG) [1], the interest started to build towards bilayer 2DEG's [2] (and for general systems with internal quantum number [3]). In the quantum Hall regime the ground state of double-layer 2DEG has been explored theoretically [2,4,5] and later experimentally [6] (and the references therein). It has been observed that in 2DEG (in this case GaAs), when the interlayer distance is small, the system at total filling fraction  $\nu_T = \nu_1 + \nu_2 = \frac{1}{2}$  ( $\nu_1, \nu_2$  being the filling fraction of each layer) and 1 forms an incompressible QHS [7–9]. The individual layers at  $\nu_T = 1$  and  $\frac{1}{2}$  have even denominator filling fractions of  $\frac{1}{2}$  and  $\frac{1}{4}$ , respectively, which are known to be compressible states. This phase is a layer-coherent phase in which the electron of one layer forms a bound state with the holes of the other layer forming excitons and spontaneously breaks the layer  $U(1)$  symmetry. We can think of layer-coherent states as either easy plane layer pseudospin ferromagnet or electron-hole bound exciton [6]. This arises from the conservation of particle number in the individual layers. Development in fabrication of high quality graphene [10,11] samples has boosted the interest in studying different structures made out of graphene and their consequences to quantum Hall. In some recent experiments involving double-layer graphene layer-coherent state has been observed [12–14]. It is possible to fabricate double-layer graphene with very small interlayer distance  $d$  ( $\sim 2$  nm) where  $d/l < 1$  ( $l$  being the magnetic length) [12–20], which was earlier difficult to achieve in GaAs systems. The separator between the graphene layers is made out of stacked hexagonal boron nitride (hBN) layers. Thus by changing the number of stacked hBN layers the interlayer interaction can be tuned

from weak to strong. This induced a huge interest in the understanding and testing of the double layers of graphene, Bernal-stacked bilayer graphene [12,18], twisted magic angle bilayer graphene [21], etc. There have been some theoretical [22–26] and experimental [27] studies to understand the Coulomb drag in double-layer graphene in zero magnetic field. In Ref. [28] it has been predicted that at higher temperature at the zero magnetic field there can be a superfluid to normal transition in double-layer graphene.

In the presence of an ultrashort-range (compared to the magnetic length  $l$ ) interaction, the Hamiltonian projected to the  $n = 0$  Landau level manifold for monolayer graphene (MLG) has  $SU(2)_{\text{spin}} \times [U(1) \times \mathbb{Z}_2]_{\text{valley}}$  symmetry in the absence of a Zeeman field [29]. There exists four different possible phases namely ferromagnet (F), charge density wave (CDW), Kekulé distorted phase (KD), and antiferromagnet (AF). AF becomes canted antiferromagnet (CAF) in the presence of Zeeman coupling [30]. The predicted phase transition from CAF to F [31–36] by changing the Zeeman coupling has been verified in the experiment [37]. This understanding of symmetry has been used to study the ground state of MLG at fractional fillings as well [38].

In the case of double monolayer graphene electron fillings of each layer ( $\nu_1$  and  $\nu_2$ ) can be controlled independently [12,13,18]. Some of the states found in these experiments can be explained using interlayer Jain composite fermion states [4], proposed for double-layer two-dimensional electron gas [13].

In this manuscript we propose the relevant symmetry in double monolayer graphene which restricts the interacting Hamiltonian to three parameters. Within the scope of this manuscript, we restrict ourselves to understanding the mean field ground state when two layers of graphene are at  $\nu_1 = \nu_2 = 0$ . We show that, for certain values of the parameters, the ground state of the system is a layer-coherent phase, which has a small magnetization proportional to the Zeeman field. Increasing the Zeeman field strength one can drive a second

\* amartya.saha@uky.edu

† ankur.das@weizmann.ac.il

order phase transition from a magnetized layer-coherent phase to the ferromagnetic phase. Here we would like to emphasize that we want to find a low energy Hamiltonian that is restricted by symmetry. We also focus on the translation invariant ground state solutions of this low energy Hamiltonian. Here we do not talk about how a specific microscopic model might give rise to the low energy effective model but only discuss the properties of the effective model itself.

We describe our assumptions, method, and findings in a few sections. In Sec. II we describe the assumptions and the Hamiltonian. After that we describe the results and the Goldstone modes in Secs. III and IV, respectively. We also discuss possible lattice models and experimental signatures in Sec. V. Then in Sec. VI we summarize our findings and describe possible application of this work.

## II. ASSUMPTIONS AND MODEL

As we are interested in the  $\nu_1 = \nu_2 = 0$  ground state, we restrict our calculations to the  $n = 0$  Landau level. When the interaction strength is much smaller than the cyclotron energy gap the Landau level mixing can be ignored, which justifies  $n = 0$  being our low energy subspace. In the weak interaction strength regime the form of the effective theory gets dictated by the symmetry (discussed below) when we integrate out the higher Landau levels. As the distance between layers is increased, the interlayer interaction will go to zero where we expect the same physics as two decoupled MLG. The valley  $U(1)$  for each layer is conserved in order to conserve the

translational symmetry in each layer separately. Here we make an additional assumption that the global spin  $SU(2)$  symmetry can be enhanced to spin  $SU(2)$  symmetry for each layer separately. For this to be the symmetry of this theory we assume that interlayer spin-spin interaction is zero (or negligible). In the absence of the interlayer tunneling it is justified that the Heisenberg term also ( $\vec{S} \cdot \vec{S}$ ) will be absent. Other than the Heisenberg a long range spin dipole-dipole interaction between layers can break the spin  $SU(2)$  symmetry in each layer to a global  $SU(2)$  symmetry. However, the spin dipole-dipole interaction falls as  $r^{-4}$ . As the distance between the layers is a few nanometers, we choose to ignore this interaction. These assumptions allow us to enhance the symmetry to spin  $SU(2)$  symmetry of each layer which allows only the intralayer  $\vec{S} \cdot \vec{S}$  interaction.

From this understanding and keeping in mind that the number of particles in each layer is fixed we propose our symmetry of the continuum model to be (in the absence of Zeeman coupling)  $[SU(2)_{\text{spin}} \otimes U(1)_{\text{valley}}]$  for each layer, a global  $(\mathbb{Z}_2)_{\text{valley}}$  and  $[U(1) \otimes \mathbb{Z}_2]_{\text{layer}}$  for the layers. This restricts the interacting part of the Hamiltonian to only three parameters. We can write the Hamiltonian as

$$H = H_0 + H_{\text{int}}, \quad (1)$$

where  $H_0$  is the one body term coming from Zeeman coupling such that

$$H_0 = -E_z(\sigma^z \otimes \tau^0 \otimes \gamma^0). \quad (2)$$

$H_{\text{int}}$ , the two body interaction term which obeys the above mentioned symmetry, is given by

$$\begin{aligned} H_{\text{int}} = & \frac{\pi l^2}{A} \sum_{\vec{q}} e^{-iq_x(k_1 - k_2 - q_y)l^2 - \frac{q_y^2 l^2}{2}} \left[ K_{xy} \sum_{i=1,2} : \bar{c}_{k_1 - q_y}^\dagger (\sigma^0 \otimes \tau^i \otimes P_L) \bar{c}_{k_1} \bar{c}_{k_2 + q_y}^\dagger (\sigma^0 \otimes \tau^i \otimes P_L) \bar{c}_{k_2} : \right. \\ & + K_z : \bar{c}_{k_1 - q_y}^\dagger (\sigma^0 \otimes \tau^3 \otimes P_L) \bar{c}_{k_1} \bar{c}_{k_2 + q_y}^\dagger (\sigma^0 \otimes \tau^3 \otimes P_L) \bar{c}_{k_2} : \\ & \left. + L_z : \bar{c}_{k_1 - q_y}^\dagger (\sigma^0 \otimes \tau^0 \otimes \gamma^3) \bar{c}_{k_1} \bar{c}_{k_2 + q_y}^\dagger (\sigma^0 \otimes \tau^0 \otimes \gamma^3) \bar{c}_{k_2} : \right]. \quad (3) \end{aligned}$$

Here  $\bar{c}_k = (c_{k,\uparrow,K,1}, c_{k,\downarrow,K,1}, c_{k,\uparrow,K',1}, c_{k,\downarrow,K',1}, c_{k,\uparrow,K,2}, c_{k,\downarrow,K,2}, c_{k,\uparrow,K',2}, c_{k,\downarrow,K',2})^T$  presents the column vector of fermionic annihilation operators,  $A$  is the area of the sample, and  $l$  is the magnetic length. The index  $k_i$  represents the guiding centers in the Landau gauge. We use the convention where  $\sigma^i, \tau^i, \gamma^i$  represents the Pauli matrices in spin, valley, and layer, respectively. Here,  $P_L = \frac{[\gamma^0 - (-1)^L \gamma^3]}{2}$  is the layer projection operator to layer  $L$ . The parameters  $K_z$  and  $K_{xy}$  arise from the intralayer interactions and are the same as the parameters  $u_z$  and  $u_\perp$ , respectively, as defined by Kharitonov in the monolayer graphene case [26]. The parameter  $L_z$  is a function of the distance between the layers ( $d$ ) which should go to zero as  $d$  becomes very large (disjoint MLG limit). Here we would like to comment that we also added a capacitance term to the Hamiltonian, which is zero when both layers have

equal fillings [39],

$$H_{\text{cap}} = \frac{g_{es} \pi l^2}{A} [\rho_1(\mathbf{q} = 0) - \rho_2(\mathbf{q} = 0)]^2, \quad (4)$$

where  $\rho_L(\vec{q})$  is the Fourier transformed electron density operator of the  $L$ th layer and  $g_{es}$  is the coupling strength of the capacitance term.

We define an order parameter  $\Delta$  matrix which specifies the HF states  $|HF\rangle$ ,

$$\langle HF | c_{k,s,\alpha,L}^\dagger c_{k,s',\alpha',L} | HF \rangle = \delta_{\vec{k},\vec{k}'} \Delta_{s'\alpha'L,s\alpha L}, \quad (5)$$

where  $s$  is the spin,  $\alpha$  is the valley, and  $L$  is the layer index. This  $\Delta$  matrix can also be thought of as a sum of projection operators of the four filled states at each momentum. The  $\Delta$  matrix completely determines the single Slater determinant states and any other order parameters, e.g., electron density,

magnetization, etc., can be calculated using it. We assume that the HF states preserve translation symmetry, i.e., the guiding centers are a good quantum number. Hence we drop the guiding center label from the  $\Delta$  matrix. Since the capacitance term is a classical term, we only keep the Hartree term and drop the Fock term. In the next section, we discuss the  $\Delta$  matrix of the different HF states.

### III. RESULTS

At  $\nu_1 = \nu_2 = 0$  there are four occupied single particle states in the spin-valley-layer space. For  $L_z \geq 0$  we find that the phase diagram is exactly the same as the phase diagram found for MLG in Ref. [30]. The energies of the phases (defined as  $E_{gs} = \langle HF | H_{\text{int}} | HF \rangle$  for the proposed HF ground state) depend on  $L_z$ . For these phases, the layer  $U(1)$  is not broken and the  $\Delta$  matrix is block diagonal in the layer index. Each of this block is a four dimensional matrix in the space of valley and spin. The four phases are as follows.

(1) Charge density wave (CDW): CDW breaks the valley  $\mathbb{Z}_2$  symmetry. At the zero Landau level, different valley indices are pinned to the sublattices. In this phase in each layer the alternate sites (A) in the lattice are occupied and the other sites (B) are left unoccupied. The  $\Delta$  matrix for this phase is

$$\Delta_{\text{CDW}} = \sigma^0 \otimes (\tau^0 + \tau^3) \otimes \gamma^0 \quad (6)$$

and the energy is

$$E_{\text{CDW}} = 2(K_z - L_z). \quad (7)$$

(2) Kekulé distorted (KD): this is a bond order phase where the valley  $U(1)$  symmetry is broken. In lattice limit the spontaneous breaking of the valley  $U(1)$  symmetry leads to the translation symmetry breaking in each layer. All the excitations of this ground state are gapped. The  $\Delta$  matrix for this phase will be

$$\Delta_{\text{KD}} = \frac{1}{2} \sigma^0 \otimes (\tau^0 + \tau^1) \otimes \gamma^0, \quad (8)$$

with energy

$$E_{\text{KD}} = 2(K_{xy} - L_z). \quad (9)$$

(3) Ferromagnet (F): this phase breaks the spin  $SU(2)$  symmetry in each layer. Similarly, the  $\Delta$  matrix and energy will be

$$\Delta_{\text{F}} = \frac{1}{2} (\sigma^0 + \sigma^3) \otimes \tau^0 \otimes \gamma^0, \quad (10)$$

$$E_{\text{F}} = -4E_z - 2(2K_{xy} + K_z + L_z). \quad (11)$$

(4) Canted antiferromagnet (CAF): this phase breaks the spin  $U(1)$  symmetry in each layer. The  $\Delta$  matrix is [35]

$$\Delta_{\text{CAF}} = \frac{1}{2} [\sin \phi (\sigma^1 \otimes \tau^3 \otimes \gamma^0) + \cos \phi (\sigma^3 \otimes \tau^0 \otimes \gamma^0) + \sigma^0 \otimes \tau^0 \otimes \gamma^0], \quad (12)$$

where  $\phi$  is given by

$$\cos \phi = \frac{E_z}{2|K_{xy}|}, \quad (13)$$

with energy

$$E_{\text{CAF}} = -4E_z - 2(2K_{xy} + K_z + L_z). \quad (14)$$

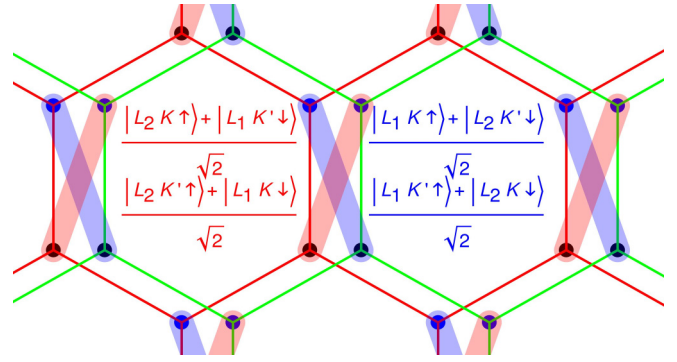


FIG. 1. Here we represent the layer-coherent (LC) phase. The layers here are color coded (green lines and red lines). As shown here the states are linear combinations of different layer indices. The corresponding states are also color coded as blue and light red.

At  $E_z = 0$  the state becomes a pure antiferromagnetic state. Increasing the Zeeman field  $E_z$  beyond  $2|K_{xy}|$  can drive a continuous phase transition from canted antiferromagnetic phase to ferromagnetic phase.

Next we come to the spacial phase of the double layer graphene. For  $L_z < 0$ , we find there exists a layer coherent phase which breaks the layer  $U(1)$  symmetry (see Fig. 2). We find the layer coherent phase both in the presence and absence of the Zeeman energy. For a nonzero Zeeman coupling, there are two parameters (and operators which are connected by the left over ground state symmetry) that

$$\Phi_L = \sigma^1 \times \tau^1 \times \gamma^1, \quad (15a)$$

$$S^z = \frac{\sigma^3 \times \tau^0 \times \gamma^0}{2}. \quad (15b)$$

The magnetic layer-coherent phase becomes the ground state at  $E_z \neq 0$  with  $\langle S^z \rangle \neq 0$ . At  $E_z = 0$  we find  $\langle S^z \rangle = 0$ , which we call the layer-coherent phase (LC) (see Fig. 1). We can

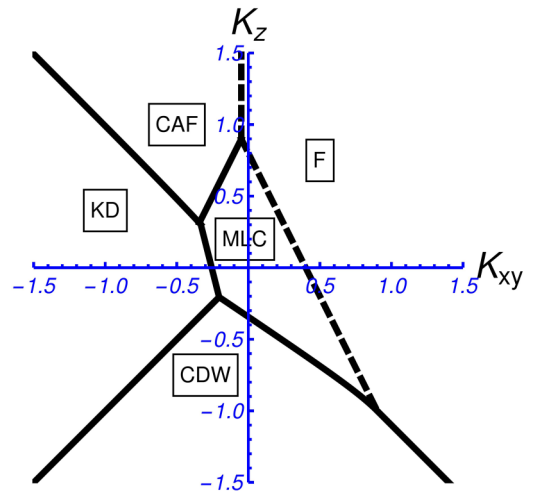


FIG. 2. Here we present the phase diagram for  $L_z = -0.5$  and  $E_z = 0.1$ . As we can see the MLC phase appears and there is a second order transition from MLC to F as marked by the broken line.

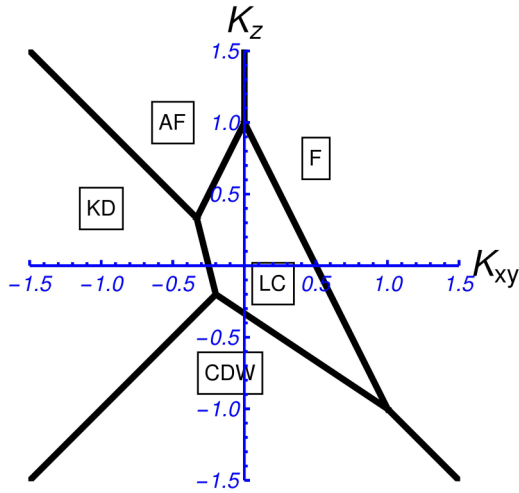


FIG. 3. Here we present the phase diagram for  $L_z = -0.5$  in the absence of Zeeman coupling. The LC phase appears near  $K_{xy} = K_z = 0$ . All the phase transitions here are first order.

write the  $\Delta$  matrix for the MLC phase as

$$\Delta_{\text{MLC}} = \frac{1}{2}[\sin \theta(\sigma^1 \otimes \tau^1 \otimes \gamma^1) + \cos \theta(\sigma^3 \otimes \tau^0 \otimes \gamma^0) + \sigma^0 \otimes \tau^0 \otimes \gamma^0], \quad (16)$$

with  $\cos \theta$  defined as

$$\cos \theta = \frac{2E_z}{|2K_{xy} + K_z + 2L_z|}. \quad (17)$$

The energy of the phase is

$$E_{\text{MLC}} = -2K_{xy} - K_z - \frac{4E_z^2}{|2K_{xy} + K_z + 2L_z|}. \quad (18)$$

Here  $\langle \Phi_L \rangle = 4 \sin \theta$  and  $\langle S^z \rangle = 2 \cos \theta$ . For  $2E_z \geq |2K_{xy} + K_z + 2L_z|$  with  $\theta = 0$ , this  $\Delta$  will represent a ferromagnetic ground state. For other values of  $\theta$  the  $\Delta$  matrix represents the MLC phase. For the zero Zeeman coupling, we have  $\cos \theta = 1 \Rightarrow \langle S^z \rangle = 0$ , a purely layer-coherent state. The phase transition from MLC to F is a second order transition (see Fig. 2). However, similar to the AF to F phase transition, the LC to F phase transition is a first order transition. Thus all phase transitions are first order at  $E_z = 0$  (see Fig. 3). The phase boundary between MLC and F changes, as we change

TABLE I. Phase boundary equations as a function of the parameters.

| Phases  | Boundary equation   |
|---------|---|
| KD,CAF  | $K_z = -K_{xy} + E_z^2/K_{xy}$  |
| KD,CDW  | $K_z = K_{xy}$  |
| F,CDW   | $K_z = -K_{xy} + E_z$   |
| F,MLC   | $K_z = -2K_{xy} - 2L_z - 2E_z$  |
| MLC,CDW | $-\frac{3K_z}{2} = (L_z + 2K_{xy} - \sqrt{(2L_z + K_{xy})^2 + 3E_z^2})$ |
| CAF,MLC | $K_z = 2(K_{xy} - L_z)$   |
| KD,MLC  | $K_z = -3K_{xy} - \sqrt{(K_{xy} - 2L_z)^2 + 4E_z^2}$                    |
| F,CAF   | $K_{xy} = -E_z/2$   |

the total Zeeman couplings at a fixed  $L_z$ . Here in Table I we represent all different phase boundaries.

#### IV. GOLDSTONE MODES

The Hamiltonian in the presence of a Zeeman term has five different  $U(1)$  symmetries coming from  $U(1)_{\text{spin}} \otimes U(1)_{\text{valley}}$  for the two layers and a layer  $U(1) \times \mathbb{Z}_2$  symmetry. For the layer diagonal phases, the presence of a gapless bulk Goldstone mode is known. The CDW phase has no gapless bulk mode. In the continuum limits it seems that the KD phase breaks a continuous symmetry but, as valley indices are momenta, it breaks lattice symmetry. Hence in this phase we will have no Goldstone modes. The F phase has spin wave mode and, at long wavelength, its gap is proportional to the Zeeman coupling strength ( $E_z$ ). As the CAF phase breaks the spin  $U(1)$  symmetry there will be a pair of gapless neutral modes in the bulk [34].

Next we discuss the new layer-coherent phase and its bulk modes. From Eq. (16) one can easily see that the ground state has the two leftover  $U(1)$  symmetries defined by operators  $\sigma^3 \otimes \tau^3 \otimes \gamma^0$  and  $\sigma^3 \otimes \tau^0 \otimes \gamma^3$ . These operations can be understood as opposite spin rotations at different valleys or different layers. In other words, these are relative valley and layer spin twists, respectively. Thus, out of five different continuous symmetries, three are broken by the ground states giving rise to three different Goldstone modes in the bulk. However, these modes will be neutral as there is a charge gap in the bulk and these excitations are similar to spin waves. We remind the readers here that the breaking of the valley part of the symmetry breaks the lattice  $C_3$  rotation about a site. This happens as the  $n = 0$  manifold the  $\mathbf{K}, \mathbf{K}'$  of each layer maps to the  $A, B$  sublattice of each layer [30]. This means we will count one extra Goldstone mode in the continuum analysis.

#### V. DISCUSSION

In this manuscript, we constructed the Hamiltonian for double-layer graphene at  $v_1 = v_2 = 0$  using symmetry principles without discussing the nature and details of the interaction at the lattice scale. The model only assumes the lattice interactions are local and thus their Fourier transform is a function independent of momentum.

In principle we can reproduce the interactions in the continuum model by projecting the microscopic Hamiltonian to the lowest Landau level. We present a very simplified example which includes the on-site Hubbard interaction ( $U_1$ ), nearest neighbor interlayer electron density-density interaction ( $U_2$ ), and an intralayer nearest neighbor spin-spin interaction ( $J$ ),

$$H_{\text{lat}} = U_1 \sum_{\substack{s_1, s_2 \\ r, L}} : n_{s_1, r, L} n_{s_2, r, L} : + U_2 \sum_{\substack{s_1, s_2 \\ r, r' \\ L_1 \neq L_2}} : n_{s_1, r, L_1} n_{s_2, r', L_2} : + J \sum_{(r, r'), L} : \vec{S}_{r, L} \cdot \vec{S}_{r', L} : \quad (19)$$

Here  $n$  is the fermion number operator and  $\vec{S}$  is the local spin operator. Though we assumed ultrashort interactions, adding finite range to these interactions does not change the symmetry of the continuum model when we project the Hamiltonian



in the zero Landau level manifold. We can write the relation between the continuum parameters in Eq. (3) in terms of the parameters of Eq. (19) as  $K_{xy} \propto -J$ ,  $K_z \propto U_1$ , and  $L_z \propto U_1/2 - U_2$ . This example shows us that it is possible for the parameter  $L_z$  to be negative. We know that the interaction between the two layers ( $U_2$ ) will increase as we reduce the distance between the layers. That means  $L_z$  can change sign as we change the distance between the layers.

We would like to emphasize here that the Hamiltonian presented here is just an example to show that, even at the simplest model at the lattice level, we can achieve the Hamiltonian in Eq. (3). Here we are not concerned with the values/signs of different parameters  $K_{xy}$ ,  $K_z$ ,  $L_z$  but showing the phases that are determined by these parameters. Modeling a generic lattice theory with physically motivated parameters and their values is an interesting study but out of the scope for the current manuscript. We hope to study a lattice microscopic model of a double-layer graphene in the future.

From Eq. (16) we can see that the states are mixtures of  $\bar{K}$ ,  $\bar{K}'$  of different layers. Near the edge the dispersion will contain two pairs of particlelike bands and another two pairs of holelike bands due to the breaking of the translation symmetry [40]. There will be a pair of counterpropagating modes only if we have identical layers near the edge of the system. Near the edge, both the valley  $U(1)$  symmetry and the layer  $U(1)$  will be broken generically due to edge mismatch. Thus the edge of a double-layer graphene will be gapped if the bulk is in MLC phase. As the states are a superposition of two different layers, there will be a drag in the two terminal measurements at least for finite temperature [16]. However, we know that there will be two pairs of counterpropagating modes at the edge for each layer in the F phase [33,37,40]. Thus, by changing the Zeeman energy with respect to the interaction energies, one can make a transition from MLC to F. This should show up in the two terminal conductance measurement [37]. It will also be interesting to measure the lattice scale structure using both the spin resolved and spin unresolved [41] tunneling electron microscope to confirm the phase directly [42,43].

## VI. SUMMARY AND OUTLOOK

Here we argued that the continuum limit of the double-layer graphene at  $\nu_1 = \nu_2 = 0$  can be assumed to have a big symmetry group that restricts the interacting part of the Hamiltonian severely to only three parameters at the  $n = 0$  Landau level. Further, we find a candidate ground state using the HF approximation that breaks the layer  $U(1)$  symmetry (generally called the MLC). We also find a second order phase transition from MLC to F as a function of Zeeman energy. We argued for a general system; the edge of the MLC will be gapped. This leads to the possible experiment to find two

terminal conductance that will change when we go from the MLC to F.

This study is just the beginning of understanding the double-layer graphene ground state in the quantum Hall regime. It was previously shown that the phase transition from CAF to F connects the bulk gapless modes of the CAF to the gapless edge modes of F [34]. We hope to study the edge theory of double-layer graphene in the future in more detail to answer the question of the phase transition from MLC to F by changing Zeeman energy.

It has been shown that if we have finite range interactions in MLG then we can have coexistence of phases [44]. Similarly, in a lattice model coexistence can also be shown by doing HF calculation in the lattice limit [45]. This explains the experimental results [41], where bond order was observed using a scanning tunneling microscope. This question may also be important in the double-layer graphene case, as we might have a similar coexistence. However, increasing the range of the interaction from ultrashort range will not change the symmetry on the theory but will only make the interaction parameters  $K_{xy}$ ,  $K_z$ ,  $L_z$  functions of  $\vec{q}$ . To understand that possibility one needs to study the lattice Hamiltonian similar to the one mentioned in Eq. (19). Furthermore, this theory can be used to explore the phase diagrams at other filling fractions in the parameter space of  $K_{xy}$ ,  $K_z$  and  $L_z$  similar to the MLG case [38]. There is also a surge of interest in understanding the BCS/BEC condensation [6,17,18,46] in double-layer graphene systems. As previously mentioned this state breaks the layer  $U(1)$  symmetry just like a superfluid state. At low enough temperatures these excitons can form a superfluid state where the interaction between the electron and hole can be tuned by tuning the  $L_z$  parameter (which depends on the interlayer separation  $d$ ).

## ACKNOWLEDGMENTS

We thank G. Murthy, E. Berg, and J. S. Hofmann for useful discussions. A.S. would like to thank the US-Israel Binational Science Foundation for its support via Grant No. 2016130 and the University of Kentucky Center for Computational Sciences and Information Technology Services Research Computing for their support and use of the Lipscomb Compute Cluster and associated research computing resources. A.D. was supported by the German-Israeli Foundation (GIF) Grant No. I-1505-303.10/2019 and the Minerva Foundation. A.D. also thanks Koshland Foundation for Koshland Fellowship, Weizmann Institute of Science, Israel Deans fellowship, and Israel planning and budgeting committee for financial support.

## APPENDIX: DETAILS OF THE TECHNIQUE

The interacting Hamiltonian in Eq. (3) can be written in a simplified form as

$$H_{\text{int}} = \frac{\pi l^2}{A} \sum_{\substack{\mathbf{q}, k_1, k_2 \\ a, b, c, d}} e^{-iq_x(k_1 - k_2 - q_y)l^2 - \frac{q_z^2 l^2}{2}} V_{a, b, c, d} : c_{k_1 - q_y, a}^\dagger c_{k_1, b} c_{k_2 + q_y, c}^\dagger c_{k_2, d} : , \quad (\text{A1})$$

where

$$V_{a,b,c,d} = K_{xy} \sum_{i=1,2} (\sigma^0 \otimes \tau^i \otimes P_L)_{a,b} (\sigma^0 \otimes \tau^i \otimes P_L)_{c,d} + K_z (\sigma^0 \otimes \tau^3 \otimes P_L)_{a,b} (\sigma^0 \otimes \tau^3 \otimes P_L)_{c,d} \\ + L_z (\sigma^0 \otimes \tau^0 \otimes \gamma^3)_{a,b} (\sigma^0 \otimes \tau^0 \otimes \gamma^3)_{c,d}. \quad (\text{A2})$$

To calculate the total HF energy  $E = \langle HF | H_0 + H_{\text{int}} | HF \rangle$  we write the average of the four-fermion term that arises in the interacting Hamiltonian  $H_{\text{int}}$  as

$$\langle HF | c_{k_1-q_y, a}^\dagger c_{k_1, b} c_{k_2+q_y, c}^\dagger c_{k_2, d} | HF \rangle = \Delta_{b,a} \Delta_{d,c} \delta_{q_y, 0} - \Delta_{d,a} \Delta_{b,c} \delta_{q_y, k_1-k_2}. \quad (\text{A3})$$

The first term gives the Hartree term and the second term is the Fock term. Using this, we can calculate the energy from the electron-electron interaction given by  $E_{\text{int}} = \langle HF | H_{\text{int}} | HF \rangle$ ,

$$E_{\text{int}} = \frac{\pi l^2}{A} \sum_{\substack{a,b \\ c,d}} \sum_{\mathbf{q}} e^{-iq_x(k_1-k_2-q_y)l^2 - \frac{q_x^2 l^2}{2}} V_{a,b,c,d} (\Delta_{b,a} \Delta_{d,c} \delta_{q_y, 0} - \Delta_{d,a} \Delta_{b,c} \delta_{k_1-q_y, k_2}) \\ = \frac{\pi l^2}{A} \sum_{a,b,c,d} V_{a,b,c,d} \left( \sum_{\substack{q_x \\ k_1, k_2}} e^{-iq_x(k_1-k_2)l^2 - \frac{q_x^2 l^2}{2}} \Delta_{b,a} \Delta_{d,c} - \sum_{\mathbf{q}, k_1} e^{-\frac{q^2 l^2}{2}} \Delta_{d,a} \Delta_{b,c} \right) \\ = \frac{1}{2N_\Phi} \sum_{a,b,c,d} V_{a,b,c,d} \left( N_\Phi^2 \Delta_{b,a} \Delta_{d,c} - \frac{N_\Phi A}{(2\pi)^2} \int_{\mathbf{q}} d\mathbf{q} e^{-\frac{q^2 l^2}{2}} \Delta_{d,a} \Delta_{b,c} \right) \\ = \frac{1}{2N_\Phi} \sum_{a,b,c,d} V_{a,b,c,d} \left( N_\Phi^2 \Delta_{b,a} \Delta_{d,c} - \frac{N_\Phi A}{2\pi l^2} \Delta_{d,a} \Delta_{b,c} \right), \quad (\text{A4a})$$

$$E_{\text{int}} = \frac{N_\Phi}{2} \sum_{a,b,c,d} V_{a,b,c,d} (\Delta_{b,a} \Delta_{d,c} - \Delta_{d,a} \Delta_{b,c}), \quad (\text{A4b})$$

where  $A$  is the area of the system and  $N_\Phi = A/(2\pi l^2)$  is the number of guiding centers in the system. Hence the total energy of the system per guiding center is

$$\frac{E}{N_\Phi} = E_z (\sigma_3 \otimes \tau_0 \otimes \gamma_0)_{ab} \Delta_{b,a} + \frac{1}{2} \sum_{a,b,c,d} V_{a,b,c,d} (\Delta_{b,a} \Delta_{d,c} - \Delta_{d,a} \Delta_{b,c}). \quad (\text{A5})$$

The first term is the Zeeman contribution and the second term comes from the electron-electron interaction.

- 
- [1] K. v. Klitzing, G. Dorda, and M. Pepper, *Phys. Rev. Lett.* **45**, 494 (1980).  
[2] T. Chakraborty and P. Pietiläinen, *Phys. Rev. Lett.* **59**, 2784 (1987).  
[3] B. I. Halperin, *Helv. Phys. Acta* **56**, 75 (1983).  
[4] J. K. Jain, *Composite Fermions* (Cambridge University Press, Cambridge, UK, 2007).  
[5] V. W. Scarola and J. K. Jain, *Phys. Rev. B* **64**, 085313 (2001).  
[6] J. Eisenstein, *Annu. Rev. Condens. Matter Phys.* **5**, 159 (2014).  
[7] M. Kellogg, J. P. Eisenstein, L. N. Pfeiffer, and K. W. West, *Phys. Rev. Lett.* **93**, 036801 (2004).  
[8] T. J. Gramila, J. P. Eisenstein, A. H. MacDonald, L. N. Pfeiffer, and K. W. West, *Phys. Rev. Lett.* **66**, 1216 (1991).  
[9] J. P. Eisenstein and A. H. MacDonald, *Nature (London)* **432**, 691 (2004).  
[10] K. S. Novoselov, A. K. Geim, S. V. Morozov, D. Jiang, M. I. Katsnelson, I. V. Grigorieva, S. V. Dubonos, and A. A. Firsov, *Nature (London)* **438**, 197 (2005).  
[11] Y. Zhang, Y.-W. Tan, H. L. Stormer, and P. Kim, *Nature (London)* **438**, 201 (2005).  
[12] J. I. A. Li, T. Taniguchi, K. Watanabe, J. Hone, A. Levchenko, and C. R. Dean, *Phys. Rev. Lett.* **117**, 046802 (2016).  
[13] J. I. A. Li, Q. Shi, Y. Zeng, K. Watanabe, T. Taniguchi, J. Hone, and C. R. Dean, *Nat. Phys.* **15**, 898 (2019).  
[14] X. Liu, Z. Hao, K. Watanabe, T. Taniguchi, B. I. Halperin, and P. Kim, *Nat. Phys.* **15**, 893 (2019).  
[15] R. V. Gorbachev, A. K. Geim, M. I. Katsnelson, K. S. Novoselov, T. Tudorovskiy, I. V. Grigorieva, A. H. MacDonald, S. V. Morozov, K. Watanabe, T. Taniguchi *et al.*, *Nat. Phys.* **8**, 896 (2012).  
[16] M. Titov, R. V. Gorbachev, B. N. Narozhny, T. Tudorovskiy, M. Schütt, P. M. Ostrovsky, I. V. Gornyi, A. D. Mirlin, M. I. Katsnelson, K. S. Novoselov, A. K. Geim, and L. A. Ponomarenko, *Phys. Rev. Lett.* **111**, 166601 (2013).  
[17] X. Liu, K. Watanabe, T. Taniguchi, B. I. Halperin, and P. Kim, *Nat. Phys.* **13**, 746 (2017).

- [18] J. I. A. Li, T. Taniguchi, K. Watanabe, J. Hone, and C. R. Dean, *Nat. Phys.* **13**, 751 (2017).
- [19] L. Britnell, R. V. Gorbachev, R. Jalil, B. D. Belle, F. Schedin, M. I. Katsnelson, L. Eaves, S. V. Morozov, A. S. Mayorov, N. M. R. Peres *et al.*, *Nano Lett.* **12**, 1707 (2012).
- [20] K. Lee, J. Xue, D. C. Dillen, K. Watanabe, T. Taniguchi, and E. Tutuc, *Phys. Rev. Lett.* **117**, 046803 (2016).
- [21] X. Liu, Z. Wang, K. Watanabe, T. Taniguchi, O. Vafek, and J. I. A. Li, *Science*. **371**, 1261 (2021).
- [22] W.-K. Tse, B. Y.-K. Hu, and S. Das Sarma, *Phys. Rev. B* **76**, 081401(R) (2007).
- [23] M. I. Katsnelson, *Phys. Rev. B* **84**, 041407(R) (2011).
- [24] N. M. R. Peres, J. M. B. L. dos Santos, and A. H. C. Neto, *Europhys. Lett.* **95**, 18001 (2011).
- [25] B. N. Narozhny, M. Titov, I. V. Gornyi, and P. M. Ostrovsky, *Phys. Rev. B* **85**, 195421 (2012).
- [26] M. Y. Kharitonov and K. B. Efetov, *Semicond. Sci. Technol.* **25**, 034004 (2010).
- [27] S. Kim, I. Jo, J. Nah, Z. Yao, S. K. Banerjee, and E. Tutuc, *Phys. Rev. B* **83**, 161401(R) (2011).
- [28] H. Min, R. Bistritzer, J.-J. Su, and A. H. MacDonald, *Phys. Rev. B* **78**, 121401(R) (2008).
- [29] J. Alicea and M. P. A. Fisher, *Phys. Rev. B* **74**, 075422 (2006).
- [30] M. Kharitonov, *Phys. Rev. B* **85**, 155439 (2012).
- [31] I. F. Herbut, *Phys. Rev. B* **75**, 165411 (2007).
- [32] I. F. Herbut, *Phys. Rev. B* **76**, 085432 (2007).
- [33] M. Kharitonov, *Phys. Rev. B* **86**, 075450 (2012).
- [34] G. Murthy, E. Shimshoni, and H. A. Fertig, *Phys. Rev. B* **90**, 241410(R) (2014).
- [35] G. Murthy, E. Shimshoni, and H. A. Fertig, *Phys. Rev. B* **93**, 045105 (2016).
- [36] A. Knothe and T. Jolicoeur, *Phys. Rev. B* **92**, 165110 (2015).
- [37] A. F. Young, J. D. Sanchez-Yamagishi, B. Hunt, S. H. Choi, K. Watanabe, T. Taniguchi, R. C. Ashoori, and P. Jarillo-Herrero, *Nature (London)* **505**, 528 (2014).
- [38] I. Sodemann and A. H. MacDonald, *Phys. Rev. Lett.* **112**, 126804 (2014).
- [39] X.-G. Wen and A. Zee, *Phys. Rev. Lett.* **69**, 1811 (1992).
- [40] G. Murthy, E. Shimshoni, and H. A. Fertig, *Phys. Rev. B* **96**, 245125 (2017).
- [41] S.-Y. Li, Y. Zhang, L.-J. Yin, and L. He, *Phys. Rev. B* **100**, 085437 (2019).
- [42] X. Liu, G. Farahi, C.-L. Chiu, Z. Papic, K. Watanabe, T. Taniguchi, M. P. Zaletel, and A. Yazdani, [arXiv:2109.11555](https://arxiv.org/abs/2109.11555).
- [43] A. Coissard, D. Wander, H. Vignaud, A. G. Grushin, C. Repellin, K. Watanabe, T. Taniguchi, F. Gay, C. Winkelmann, H. Courtois *et al.*, [arXiv:2110.02811](https://arxiv.org/abs/2110.02811).
- [44] A. Das, R. K. Kaul, and G. Murthy, [arXiv:2109.07515](https://arxiv.org/abs/2109.07515).
- [45] A. Das, Ph.D. thesis, University of Kentucky, Lexington, 2020, [https://uknowledge.uky.edu/physastron\\_etds/70/](https://uknowledge.uky.edu/physastron_etds/70/).
- [46] X. Liu, J. I. A. Li, K. Watanabe, T. Taniguchi, J. Hone, B. I. Halperin, P. Kim, and C. R. Dean, [arXiv:2012.05916](https://arxiv.org/abs/2012.05916).